15

Production and accumulation of isotopically pure helium-4 for ultracold neutron source

© V.A. Lyamkin,[1] A.P. Serebrov,[1] A.O. Koptyukhov,[1] D.V. Prudnikov,[1] G.O. Borodinov,[1] A.A. Nedolyak,[1] P.A. Hazov,[1] A.V. Sirotin,[1,2] A.N. Salyuk[3]

[1]St. Petersburg Nuclear Physics Institute, National Research Center Kurchatov Institute, Gatchina, Russia
[2]ITMO University, St. Petersburg, Russia
[3]V.I. Il'ichev Pacific Oceanological Institute, Far Eastern Branch, Russian Academy of Sciences, Vladivostok, Russia
e-mail: lyamkin_va@pnpi.nrcki.ru

Received November 17, 2024
Revised February 6, 2025
Accepted February 9, 2025

A high-intensity ultracold neutron source (UCN) is being created at the NRC „Kurchatov Institute"— PNPI. It is going to be placed at the PIK reactor, for scientific research in the field of physics of fundamental interactions. The UCN source will use superfluid helium, which will make it possible to achieve a UCN density of $2.2 \cdot 10^3$ cm^{-3}. To achieve these parameters, the commercial helium used as a converter has been purified from the helium-3 isotope by 3 orders of magnitude. Due to this it became possible to increase the neutron storage time in helium from 3.1 to 38.6 s. The helium was purified using a superleak filter made of pressed Al_2O_3 powder. As a result of this work, 43 m^3 of isotopically pure ^{4}He was produced and stored

Keywords: ultracold neutrons, superleak helium, neutron EDM, PIK reactor, mass spectrometry.

DOI: 10.61011/TP.2025.06.61391.423-24

Introduction

Ultracold neutrons (UCN) are used to study the physics of fundamental interactions. Because of their small energy — about 10^{-7} eV — these neutrons have a unique feature — they can be stored in enclosed material and/or magnetic traps [1,2]. This feature enables to study the properties of the neutron itself. Currently, experiments are being conducted using UCN to search for the electric dipole moment (EDM) of a neutron [3] and measure the lifetime of a free neutron [4].

The accuracy of experiments using UCN largely depends on the power of sources of this type of neutrons. For over half a century of the experiments with UCN, many different UCN sources have been provided, which made it possible to increase the neutron density by 8 orders of magnitude [5]. The main method of producing high UCN fluxes was the use of a low-temperature converter: beryllium at 20 K, liquid hydrogen or deuterium at 20 K, solid deuterium at 5 K.

Today high UCN densities may be realized with the use of solid deuterium [6–7] or superfluid helium [8–10]. Solid deuterium is used primarily in the so-called spallation neutron sources, mainly because of the possibility of deuterium cooling in the absence of heat influx from the neutron beam. UCN source based on superfluid helium is good for stationary neutron sources, where large UCN densities can be generated in a constant neutron flux in the absence of absorption in superfluid helium.

In 2020, it started implementation of a program for creating the instrument experimental base for the PIK reactor [11]. The PIK reactor is one of the world's most powerful high-current neutron sources. Maximum design thermal capacity of the reactor is 100 MW. A project to create a high-flow UCN source based on superfluid helium has been proposed and is currently being implemented at this stationary reactor [12–14].

Although superfluid helium is transparent to UCN, nevertheless, there are mechanisms in the source that lead to losses o neutrons. In general, the storage time of UCN in the source chamber can be estimated as $\tau_{\text{UCN}}^{-1} = \tau_{4\text{He}}^{-1} + \tau_w^{-1} + \tau_n^{-1} + \tau_a^{-1}$, where $\tau_{4\text{He}}^{-1}$ — losses in superfluid helium due to the excitation of phonons and rotons, τ_w^{-1} — losses due to interaction with the walls of the source chamber, τ_n^{-1} — losses due to the lifetime of free neutrons, τ_a^{-1} — losses during neutron absorption by impurities contained in superfluid helium.

According to [15], to estimate the influence of possible interactions at a temperature below 1.95 K the dependence $\tau_{4\text{He}}^{-1} = BT_{\text{He}}^7$ may be used where $B \approx 7.6 \cdot 10^{-3}\,\text{s}^{-1}\text{K}^{-7}$ — double-phonon scattering coefficient. Thus , at $T = 1.1$ K $\tau_{4\text{He}}^{-1} = 68$ s.

Losses when interacting with the walls of the source chamber can be estimated as $\tau_w = \tau_l/\delta$, where τ_l is the time between two impacts, and $\delta = 3 \cdot 10^{-4}$ is the probability of UCN losses when interacting with the wall of the source chamber with sprayed ^{58}Ni. For our UCN source chamber configuration we get$\tau_w = 0.032/3 \cdot 10^{-4} = 107$ s.

Determination of the lifetime of a free neutron is still the subject of a number of experiments, including those planned for PIK reactor. However, according to PDG this value makes $\tau_n = (878.4 \pm 0.5)$ s [16].

The only source of neutron absorption in the superfluid helium is helium-3 isotope which is naturally found in commercial A helium. Despite the fact that the share of isotope ^{3}He in commercial helium is very small — about 10^{-6} percents, UCN absorption cross-section by helium-3 is very high. The thing is that the cross section of any nuclear reaction caused by sufficiently slow neutrons is inversely proportional to their velocity (this ratio is called the „law 1/v “). Thus, for UCN $\sigma_{abs}(\mathrm{UCN}) = (5300\,\mathrm{barn} \cdot 2200\,\mathrm{m/s})/6\,\mathrm{m/s} = 1.94 \cdot 10^6$ barn, where 5300 barn — absorption cross-section for thermal neutrons, and 2200 and 6 m/s — velocities of thermal and ultracold neutrons, respectively.

Thus, absorption losses in ^{3}He may be estimated as $\tau_a^{-1} = N\sigma_{abs}(\mathrm{UCN})v(\mathrm{UCN})$, where $N = 2.5 \cdot 10^{28} R_{3\mathrm{He}}$ — nuclear concentration of ^{3}He in the chamber, $[\mathrm{m}^{-3}]$, and $R_{3\mathrm{He}}$ — share of helium-3 in the mixture (absolute). Hence we have: $\tau_a = 3.4$ s at $R = 10^{-8}$; $\tau_a = 344$ s at $R = 10^{-10}$; $\tau_a = 34\,000$ s at $R = 10^{-12}$.

Summarizing all of the above, we have the following estimate of the lifetime of UCN in the UCN source chamber:

- $\tau_{\mathrm{UCN}} = 3$ s for $R = 10^{-8}$;
- $\tau_{\mathrm{UCN}} = 35$ s for $R = 10^{-10}$;
- $\tau_{\mathrm{UCN}} = 40$ s for $R = 10^{-12}$.

It becomes obvious that it is impossible to use natural helium for fabrication of UCN, since the presence of helium-3 isotope in it leads to the loss of most of the neutrons. For the effective operation of UCN source, commercial helium shall be purified from ^{3}He by 2–4 orders of magnitude from the initial value. Further purification of helium does not make much practical sense, since the losses associated with heating the UCN in helium at a temperature of 1.1K are prevailing.

1. Superleak filter

Commercial helium on the market contains two isotopes: ^{3}He and ^{4}He. These two isotopes have extremely low boiling points at atmospheric pressure: 3.19 K for ^{3}He and 4.22 K for ^{4}He. In general, in the liquid phase, they manifest themselves as ordinary liquids with low viscosity, but at a temperature of 2.17 K, the liquid ^{4}He undergoes a transition to the so-called superfluid state. It is worth noting that helium-3 is also capable of transitioning to a superfluid state, but for it the thermophysical parameters of the transition are more difficult to achieve: at a pressure of 34 kPa transition occurs at a temperature below 2.6 mK. Thus, at temperatures of 1–2 K, only helium-4 isotope is in the superfluid state, while helium-3 is in the normal state. The method of isotopic purification of helium using a so-called superleak filter (superleak) [17] is based on this fact.

The superleak filter is a steel cylinder with pressed ultrafine aluminum oxide powder with a fraction of 50 nm. At the same time, the filter turns out to be so dense that it passes only the superfluid component of helium through itself. Thus, by installing a filter in front of a certain container and directing helium flux at a temperature of 1–2 K through it, we can fill the container exclusively with isotopically pure helium-4 (IPH).

Figure 1. Pressing of one layer of Al_2O_3.

The superleak filter was made by layer-by-layer pressing of small portions of powder inside a thick-walled cylindrical stainless steel case (12X18H10T) with an outer diameter of 22 mm and a height of 79 mm. The pressing of powder in thin layers (height 2–3 mm), combined with a step-by-step density control in the layer was aimed at ensuring uniformity of the filter density in height. Here, the filter diameter was 8 mm.

A typical operation for pressing a single layer is as follows: the mass and height of the clogged filter are measured, the filter is placed on a pallet and filled with powder Al_2O_3, the powder is pressed by a hydraulic press with a force of three tons (Fig. 1), the measurement is performed the weight and height of the filter after pressing.

This cycle is repeated until the case is completely filled with powder. As a result of fabrication of the superleak filter, 24 operations were performed to press aluminum oxide powder into it. The average density of aluminum oxide layers in the superleak filter was (2.39 ± 0.08) g/cm^3.

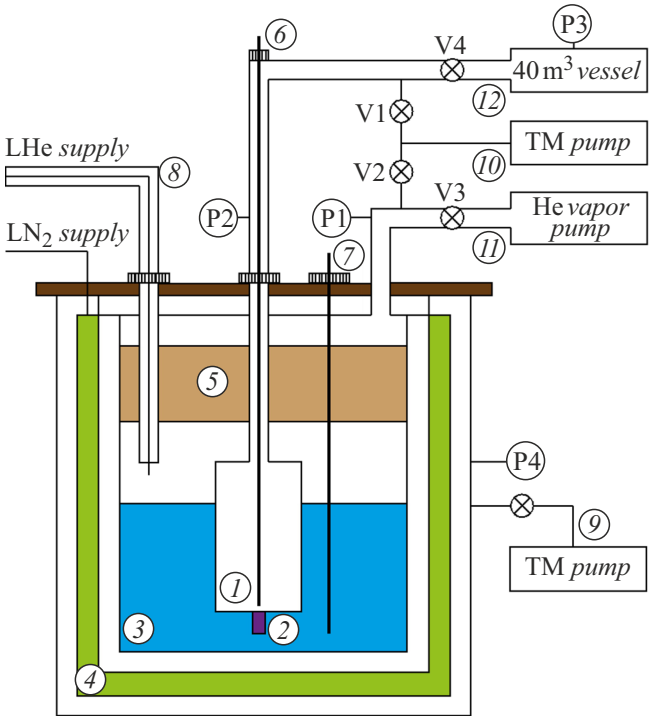

Figure 2. Schematic diagram of the setup (comments in the text).

2. Process system for buildup and storage of IPH-4

A schematic diagram and a photo of the experimental setup for the production time of IPH are shown in Fig .2, 3, respectively. A two-liter container *1* with a superleak filter *2* installed using an indium seal is placed inside the helium bath of the cryostat *3*. The helium bath *3* is surrounded by a heat shield *4* filled with liquid nitrogen. The radiative heat flow to liquid helium from the warm cryostat lid is reduced due to the multilayer thermal insulation *5*. Control and measuring devices (instrumentation) consisting of helium NbTi level gauge AMI and CERNOX CX-1030-AA thermal sensor —*6* and *7* were introduced into the cryostat tank and bath, respectively. In addition to sensors, a heater is installed in the tank — TBO resistor with a resistance of 100 Ω. Liquid helium is supplied and vapor is discharged using a cryogenic pipeline *8*. Two turbomolecular pumps are connected to the cryostat: for pumping out the vacuum casing of the cryostat and for pumping out working helium volumes *10*. The temperature of liquid helium declines from 4.2 to 1.3 K due to pumping of helium vapor using vacuum pump system EDWARDS HV30000 with a total capacity of 3 g/s. RD-10 receivers with a volume of 10 m^3 each are connected to the system for collection and storage of IPH *12*. Before starting operation, the receiver is pumped out to a pressure of 0.2 Pa. The scheme below also shows basic manual valves: V1, V2, V3, V4 and pressure sensors P1, P2, P3, P4.

In general, the point is that the pre-pumped tank *1* is located in a bath with superfluid helium *3* and is filled with isotopically pure helium-4 through the superleak filter. Further this helium may be evaporated and directed to receivers RD-10.

Further in the text, the tank with an isotopic purehelium-4 *1* will be called SOURCE, and the cryostat bath *3* — HEX.

3. Obtaining of IPH

3.1. Preparation

Previously, the receivers RD-10, SOURCE, HEX and communicating pipelines are pumped out to $P2 = P3 = 0.2$ Pa using a turbomolecular pump *10*. The vacuum case of cryostat is pumped out to $P4 = 0.02$ Pa. Next, liquid nitrogen is poured into the nitrogen screen and maintained at a maximum level throughout the experiment, which cools the cryostat's heat shield to 80 K. After pumping out of HEX/SOURCE is stopped (having closed V1/V2) 30 l of pure helium is poured into HEX tank.

3.2. Filling of receivers up to $P = 90$ Pa

When the helium vapor pumping system is turned on *11*, the temperature of helium in HEX tank decreases to 1.3 K. When crossing λ-point (at $T = 2.71$ K) a component of the superfluid helium starts to emerge in HEX. The superfluid helium, passing through the superleak, enters a highly pumped tank with a pressure below the pressure of saturated helium vapor. As a result, this helium instantly evaporates and its vapors cool the thermal sensor, which is located directly at the outlet of the superleak filter. This is detected by the temperature sensor in SOURCE tank— decline from 80 to 2−4 K. After 40 min, the temperature in HEX is detected at 1.23 K, and the level gauge shows an increase in the level of liquid helium in SOURCE. The pressure in SOURCE at this time is $P2 = 90$ Pa, which corresponds to the pressure of saturated helium vapor at 1.21 K. Thus, at the moment when pressure in the receivers is compared with pressure of saturated vapor at the current temperature of helium, the process of accumulation of liquid helium in SOURCE begins.

3.3. Filling of receivers up to $P = 52.5$ kPa

According to theoretical concepts, confirmed by numerous experiments, the flow of helium through a superleak filter is possible under the influence of a temperature gradient (thermomechanical effect). At small gradients, the filter performance is described by the linear dependence of the mass flow on the released power $m = \frac{Q}{ST}$, where m — mass flow, Q — released power, T — temperature of liquid helium, S — its entropy at a temperature of T. When a certain critical value Q is reached, depending on the individual characteristics of the filter, a subcritical (turbulent) mode occurs. At the same time, there is an increase in the flow rate m with higher Q, associated

Figure 3. SOURCE vessel (in the left) and cryostat for obtaining IPH (in the right).

with the achievement of a critical velocity of the superfluid component in the filter pores.

After liquid helium began to appear in SOURCE, a heating power of 1–12.5 W is applied to the heater in the tank. Under the influence of thermomechanical effect, helium flows from HEX to SOURCE, where, due to the same thermal load, it evaporates and fills the RD-10 receivers. In our case helium flux doesn't depend on the amount of heat load — thus we are dealing with a supercritical superleak operation. The helium flux through this filter was 1.25 g/s, which, with a filter diameter of 8 mm, corresponds to a specific flow of 2.5 g/(cm^2·s).

The system operation schedule during the first launch and the operating time of the first IPH are shown in Fig. 4. The readings from the level gauges are limited by the sensor length — 35 cm.

According to the Langmuir model, the gas flow during condensation is determined by the expression $G_{con} = \frac{N_a P}{\sqrt{2\pi MRT}} AkT$, where P — pressure above the liquid surface, A — surface area of helium, T — temperature of helium, M — molar mass of helium, N_a, k, R — physical constants. The vaporized gas flow is $G_{ev} = r \cdot Q_{heater}$, where r is the heat of helium evaporation, and Q is the power on the heater. To fill the receivers, it is necessary that $G_{ev} > G_{con}$, otherwise the reverse process occurs — condensation of helium from the receivers into SOURCE. When the receivers are filled, the pressure $P2$ in the system rises, and for further evaporation of helium, it is necessary to increase the power on the heater. Heat is removed from the SOURCE through a limited surface area in the HEX, where this heat is removed by pumping out helium vapor. Accordingly, an increase in the heater power leads to a rise in the temperature of helium in the SOURCE. At a certain power, the temperature rises above λ- point, which leads to „closure of the" superleak filter — there is no superfluid component in helium. In our case it occurred at $Q = 12.5$ W and $P = 52.5$ kPa.

3.4. Filling of receivers up to $P = 107.5$ kPa

When pressure in the receivers reached $P = 52.5$ kPa, it was impossible to simultaneously supply helium from HEX to the SOURCE and vaporize this helium from the SOURCE to the receivers. In this regard, it was decided to switch to a two-stage mode of filling the receivers:

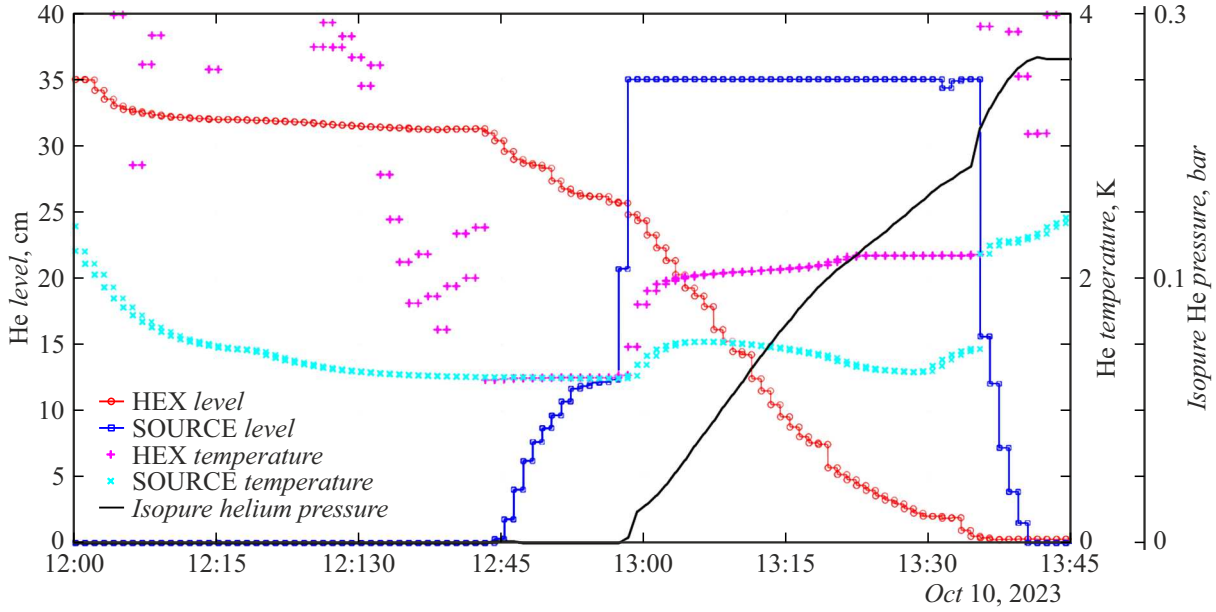

Figure 4. First IPH in receiver RD-10.

1) receivers RD-10 are isolated from the SOURCE by closing V4. Helium from HEX is poured into the SOURCE by means of thermomechanical effect at low Q on the heater;

2) V4 opens and the heater power rises to $Q = 12.5$ W. Helium starts to evaporate from SOURCE into receivers. Helium temperature in the SOURCE rises higher than 2.71 K — superleak filter „closes“, helium from HEX doesn't go to the SOURCE;

3) return to the first clause: the gate V4 closes and the heater thermal load reduces. Temperature in the SOURCE decreases below λ-point, the superleak filter„opens“, and helium from HEX goes to the SOURCE.

As a result of nine such iterations, the receivers were filled with isotopically pure helium to a pressure of $P3 = 107.5$ kPa. The total number of IPH makes 43 m^3. The last 4 iterations (filling/evaporation of helium to/from SOURCE) are shown in Fig. 5.

In our case, it was not possible to replenish helium HEX during filling of the receivers. For filling, standard helium liquefier Linde L-280 is used operating at a pressure of 0.12 MPa, while a pressure of saturated helium vapor of the order of $P2 = 200$ Pa is maintained during filling of the receivers in HEX. Thus, after helium in HEX ran out, we stopped work, closed the receivers and started over: we pumped out the SOURCE and HEX, poured helium into HEX. To get 43 m^3 of IPH we required 6 iterations. In total 176 l of liquid helium was poured into HEX.

4. Analysis of helium obtained during operation

IPH was analyzed in the FSBI „Ilyichev Pacific Oceanological Institute“ using HELIX SFT Static Vacuum Mass Spectrometer (Thermo Scientific, USA). The dependences of current of the Faraday detector (FD) and current of the electron multiplier (EM) were registered during measurement of samples of commercial helium (CH) and IPH (Fig. 6). The numbers on the graph show the ratio of peaks $R_{34} = {}^3\mathrm{He}/{}^4\mathrm{He}$, taking into account the efficiency of detecting EM ions ^{3}He $\varepsilon = 0.82$. For commercial helium the isotope ratio $R_{34} = 1.52 \cdot 10^{-8}$ ($\sigma = 6.5\,\%$) was obtained which corresponded to the atmospheric ratio $R_a = ({}^3\mathrm{He}/{}^4\mathrm{He})/({}^3\mathrm{He}/{}^4\mathrm{He})_{\mathrm{atm}} = 0.011$.

The total averaging curve of several peaks (thick line) and the current scan (thin light line) are shown for the IPH (Fig. 6, right). To improve sensitivity, the IPH sample was increased by an order of magnitude in volume, and to measure low ion counting rates ^{3}He, the integration time was 67 s with a very long total sample analysis time — more than 240 min. Each of these parameters and minimal background and very long static operation time are provided by the unique characteristics of our MS. A further increase in the size of IPH sample leads to a complete overlap of ${}^3\mathrm{He}^+$ peak with the center of mass 3.016 u by the left edge of the growing combined peak ($\mathrm{HD}^+ + \mathrm{H}_3^+$) and loss of resolution.

The ion current ${}^4\mathrm{He}^+ = 9292 \cdot 58 \approx 539\,000$ fA due to an overload of FD at a current of more than 50,000 fA was estimated by repeated measurement of 1/58 of the fraction of helium contained in the mass analyzer.

The time course of the measurement of ^{3}He ultrapure helium (Fig. 7) shows that almost all ^{3}He recorded in MS occurs in the flow during measurement, and the probable value of current ^{3}He in IPH sample at the time of admission in MS is $\sim 10 \cdot 10^{-6}$ fA, and isotopic ratio $R_{34} = 10^{-5}/539\,000/0.82 = 2.26 \cdot 10^{-11}$ (5 times lower than the current of the averaged signal $^3\mathrm{He} = 50 \cdot 10^{-6}$ fA

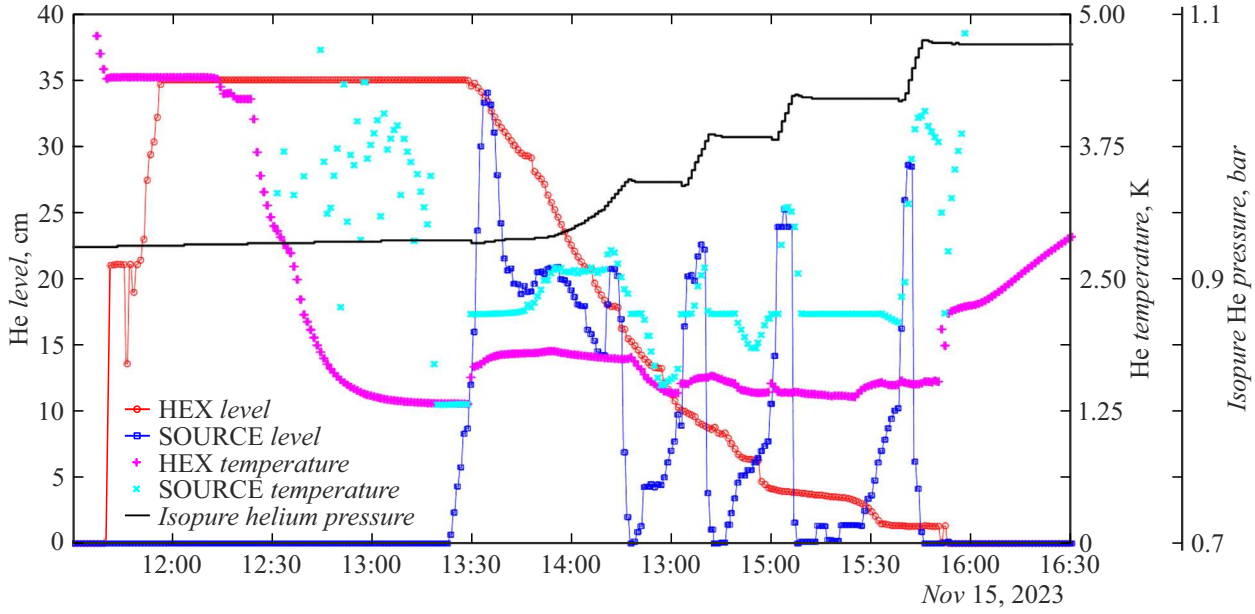

Figure 5. Process of IPH receivers filling up to $P = 1.075$ bar.

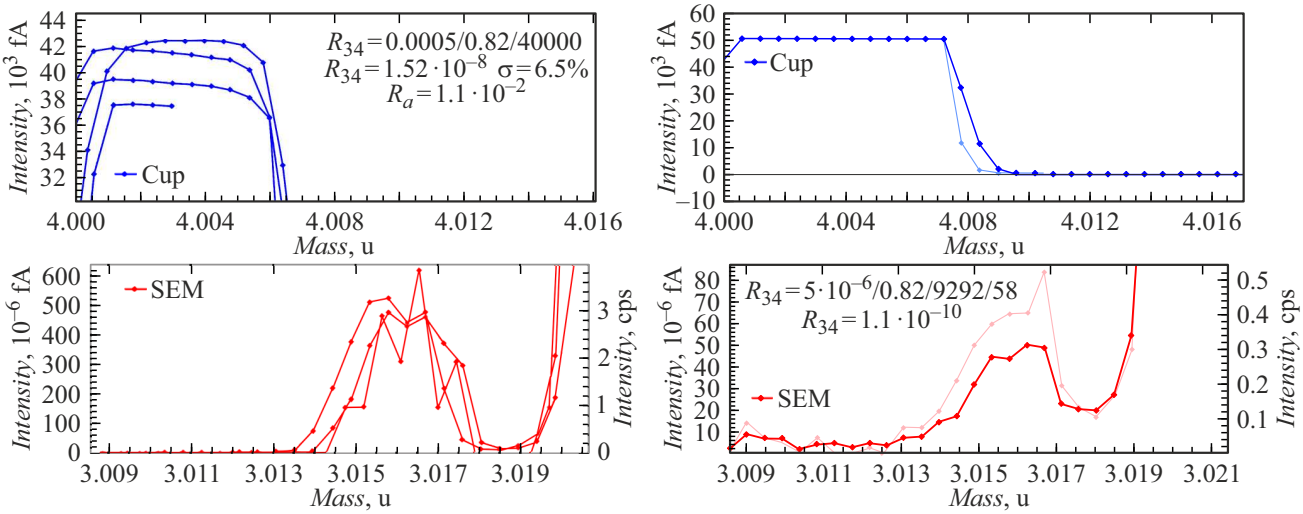

Figure 6. Analysis of helium on mass-spectrometer HELIX SFT (in the left — CH, in the rights — IPH).

in Fig. 6, which corresponds to the value $R_{34} = 1.1 \cdot 10^{-10}$). Our mass spectrometry method for measuring low isotopic ratios of helium will be described in more detail in a separate article, which is being prepared for publication.

Thus, the content of ^{3}He in purified helium is $2 \cdot 10^{-11}$, which gives $\tau_a = 1718$ s, which is significantly higher than the storage time of a free neutron. The lifetime of UCN, in its turn, will reach $\tau_{\text{UCN}} = 38.6$ s.

Conclusion

A new source of UCN for the PIK reactor based on superfluid helium required the development of technology and the creation of a complex for purifying commercial helium from isotope impurities ^{3}He. The technology used the feature of the flow of only superfluid component of helium through a superleak filter made of pressed powder Al_2O_3. Helium was purified at a temperature of 1.3 K — significantly higher temperature 2.6 mK, at which ^{3}He starts to transform into superfluid phase.

A superfluid filter made of pressed powder Al_2O_3 showed a high degree of purification of commercial helium from helium-3 isotope. It was used to prepare and pump 43 m^3 of isotope-pure ^{4}He. The analysis of helium from the receivers on a mass spectrometer showed that the value of ^{3}He was reduced by 3 orders of magnitude: from 10^{-8} to $2 \cdot 10^{-11}$. The lifetime of neutrons in purified helium is estimated at 39 s, while in commercial helium this value does not exceed 3 s.

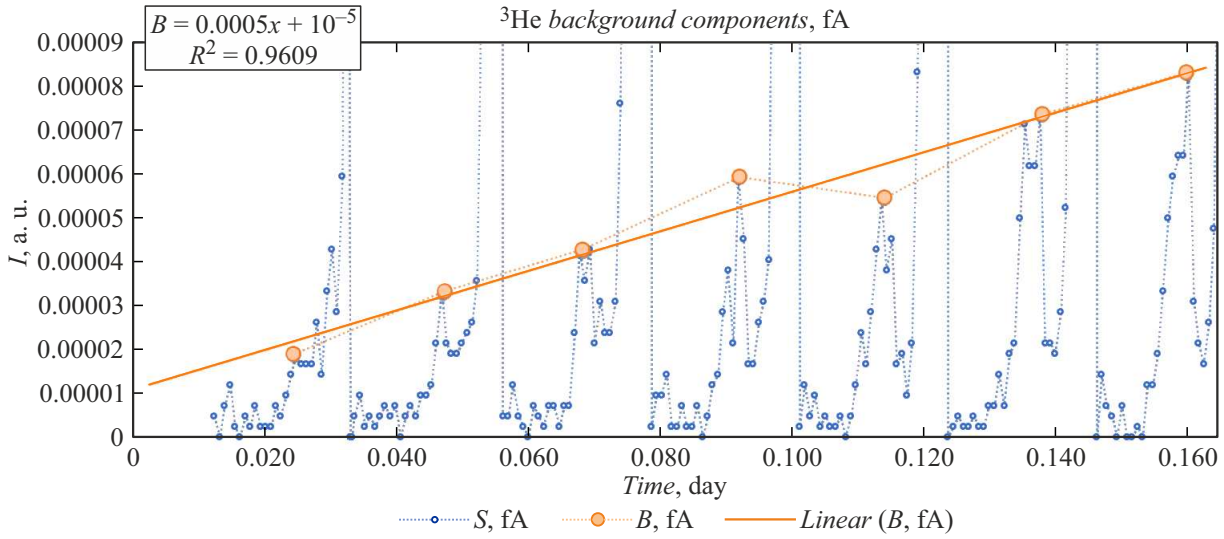

Figure 7. Time measurement of ^{3}He IPH.

This isotopically purified ^{4}He will be used for a new source of UCN based on superfluid helium in PIK reactor. The isotopic purity of helium will significantly increase the lifetime of a neutron in the source and achieve record UCN densities in experimental facilities up to 200 cm^{-3}.

A superleak filter manufactured using our technology and helium isotopic purification system will be included in the technological complex of UCN source at PIK reactor to replenish the supply of ^{4}He in the future.

Acknowledgments

The authors would liketo thank K.O.Keshishev and S.T.Boldarev, employees of Kapitsa Institute of Physical Problems, for their advice and discussion of technology for purifying helium using a superfluid filter.

Funding

This study was supported financially by the Russian Science Foundation (grant No. 23-72-10007, https://rscf.ru/project/23-72-10007/.

Conflict of interest

The authors declare that they have no conflict of interest.

References

[1] Ya.B. Zeldovich. Sov. Phys. JETP, **9** (6), 1389 (1959).
[2] V.V. Vladimirskii. Sov. Phys. JETP, **12** (4), 740 (1961).
[3] C. Abel, S. Afach, N.J. Ayres, C.A. Baker, G. Ban, G. Bison, K. Bodek, V. Bondar, M. Burghoff, E. Chanel, Z. Chowdhuri, P.-J. Chiu, B. Clement, C.B. Crawford, M. Daum, S. Emmenegger, L. Ferraris-Bouchez, M. Fertl, P. Flaux, B. Franke, A. Fratangelo, P. Geltenbort, K. Green, W.C. Griffith, M. van der Grinten, Z.D. Grujić, P.G. Harris, L. Hayen, W. Heil, R. Henneck, V. Hélaine, N. Hild, Z. Hodge, M. Horras, P. Iaydjiev, S.N. Ivanov, M. Kasprzak, Y. Kermaidic, K. Kirch, A. Knecht, P. Knowles, H.-C. Koch, P.A. Koss, S. Komposch, A. Kozela, A. Kraft, J. Krempel, M. Kuźniak, B. Lauss, T. Lefort, Y. Lemière, A. Leredde, P. Mohanmurthy, A. Mtchedlishvili, M. Musgrave, O. Naviliat-Cuncic, D. Pais, F.M. Piegsa, E. Pierre, G. Pignol, C. Plonka-Spehr, P.N. Prashanth, G. Quéméner, M. Rawlik, D. Rebreyend, I. Rienäcker, D. Ries, S. Roccia, G. Rogel, D. Rozpedzik, A. Schnabel, P. Schmidt-Wellenburg, N. Severijns, D. Shiers, R. Tavakoli Dinani, J.A. Thorne, R. Virot, J. Voigt, A. Weis, E. Wursten, G. Wyszyński, J. Zejma, J. Zenner, G. Zsigmond. Phys. Rev. Lett., **124** (8), 081803 (2020). DOI: 10.1103/PhysRevLett.124.081803
[4] F.M. Gonzalez, E.M. Fries, C. Cude-Woods, T. Bailey, M. Blatnik, L.J. Broussard, N.B. Callahan, J.H. Choi, S.M. Clayton, S.A. Currie, M. Dawid, E.B. Dees, B.W. Filippone, W. Fox, P. Geltenbort, E. George, L. Hayen, K.P. Hickerson, M.A. Hoffbauer, K. Hoffman, A.T. Holley, T.M. Ito, A. Komives, C.-Y. Liu, M. Makela, C.L. Morris, R. Musedinovic, C. O.Shaughnessy, R.W. Pattie Jr., J. Ramsey, D.J. Salvat, A. Saunders, E.I. Sharapov, S. Slutsky, V. Su, X. Sun, C. Swank, Z. Tang, W. Uhrich, J. Vanderwerp, P. Walstrom, Z. Wang, W. Wei, A.R. Young (UCNτ Collaboration). Phys. Rev. Lett., **127** (16), 162501 (2021). DOI: 10.1103/PhysRevLett.127.162501
[5] A.P. Serebrov, V.A. Lyamkin. J. Neutron Res., **24** (2), 145 (2022). DOI: 10.3233/JNR-220007
[6] B. Lauss, B. Blau. Sci. Post Phys. Proceed., **5**, 004 (2021). DOI: 10.21468/SciPostPhysProc.5.004
[7] T.M. Ito, E.R. Adamek, N.B. Callahan, J.H. Choi, S.M. Clayton, C. Cude-Woods, S. Currie, X. Ding, D.E. Fellers, P. Geltenbort, S.K. Lamoreaux, C.Y. Liu, S. MacDonald, M. Makela, C.L. Morris, R.W. Pattie Jr., J.C. Ramsey, D.J. Salvat, A. Saunders, E.I. Sharapov, S. Sjue, A.P. Sprow, Z. Tang, H.L. Weaver, W. Wei, A.R. Young. Phys. Rev. C, **97** (1), 012501 (2018). DOI: 10.1103/PhysRevC.97.012501

[8] K.K.H. Leung, G. Muhrer, T. Hügle, T.M. Ito, E.M. Lutz, M. Makela, C.L. Morris, R.W. Pattie, A. Saunders, A.R. Young. J. Appl. Phys., **126** (22), (2019).
[9] O. Zimmer, R. Golub. Phys. Rev. C, **92**, 015501 (2015). DOI: 10.1103/PhysRevC.92.015501
[10] J. Martin, B. Franke, K. Hatanaka, S. Kawasaki, R. Picker. Nucl. Phys. News, **31** (2), 19 (2021). DOI: 10.1080/10619127.2021.1881367
[11] M.B. Kovalchuk, V.V. Voronin, S.V. Grigoryev, A.P. Serebrov. Crystallography Reports, **66** (2), 195 (2021). DOI: 10.1134/S1063774521020061
[12] A.P. Serebrov, V.A. Lyamkin, A. K. Fomin, M.S. Onegin. Tech. Phys., **67** (6), 763 (2022). DOI: 10.21883/TP.2022.06.54425.21-22
[13] A.P. Serebrov, A.K. Fomin, M.S. Onegin, A.G. Kharitonov, D.V. Prudnikov, V.A. Lyamkin, S.A. Ivanov. Tech. Phys. Lett., **40** (1), 10 (2014). DOI: 10.1134/S1063785014010118
[14] A.P. Serebrov. Phys.-Usp., **58** (11), 1074 (2015). DOI: 10.3367/UFNe.0185.201511c.1179
[15] K.K.H. Leung, S. Ivanov, F.M. Piegsa, M. Simson, O. Zimmer. Phys. Rev. C, **93** (2), 025501 (2016). DOI: 10.1103/PhysRevC.93.025501
[16] ParticleDataGroup. *Review of Particle Physics* (Oxford University Press, Oxford, 2022)
[17] H. Yoshiki, H. Nakai, E. Gutsmiedl. Cryogenics, **45** (6), 399 (2005). DOI: 10.1016/j.cryogenics.2005.01.007

Translated by T.Zorina